Journal of Medicinal Chemistry

Article

pubs.acs.org/jmc

A Soluble Bis-Chelated Gold(I) Diphosphine Compound with Strong Anticancer Activity and Low Toxicity

Yanli Wang,[‡,∥] Minyu Liu,[†,§,∥] Ran Cao,[‡] Wanbin Zhang,[†] Ming Yin,[†] Xuhua Xiao,[§] Quanhai Liu,*[,§] and Niu Huang*[,‡]

[†]School of Pharmacy, Shanghai Jiao Tong University, 800 Dong Chuan Road, Shanghai 200240, China

[‡]National Institute of Biological Sciences, Beijing, 7 Science Park Road, Zhongguancun Life Science Park, Beijing 102206, China

[§]Department of Pharmacology, Shanghai Institute of Pharmaceutical Industry, 1111 Zhong Shan Bei Yi Road, Shanghai 200437, China

Supporting Information

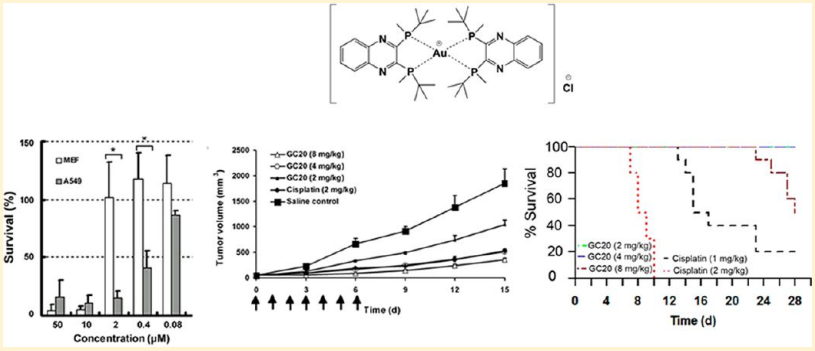

ABSTRACT: Gold-containing compounds have shown anticancer potential, but their clinical applications have been severely limited by poor stability and high toxicity in vivo. Here, we report a novel soluble bis-chelated gold(I)−diphosphine compound (GC20) with strong anticancer activity and low toxicity. GC20 shows strong antiproliferation potency against a broad spectrum of cancer cell lines including cisplatin-resistant cancer cells ($IC_{50} \approx 0.5\ \mu M$) and significantly reduces tumor growth in several tumor xenografts in mouse models at doses as low as 2 mg/kg. Studies of its mechanism revealed that GC20 specifically inhibits the enzymatic activity of thioredoxin reductase by binding to selenocysteine residue, without targeting other well-known selenol and thiol groups contained in biomolecules. Remarkably, in animal studies GC20 was shown to be well tolerated even at the high dose of 8 mg/kg. Our results strongly suggest that GC20 represents a promising candidate for the development of novel anticancer drugs.

INTRODUCTION

Metal-containing compounds such as cisplatin and carboplatin[1] have long been used clinically as potential cancer chemotherapy agents.[2−4] However, the therapeutic effects of these agents are not universal and their side effects, most noticeably systemic toxicity, have limited their widespread application. Moreover, acquired resistance in long-term treatment has frequently been observed, which might be partially attributed to irreversible consumption by enhanced glutathione (GSH) content.[1,4−6] Nevertheless, the success of cisplatin has stimulated a broad interest in the exploration of compounds containing metals, such as nickel, ruthenium, and gold, as potential anticancer agents with unique pharmacologic, kinetic, and geometric properties.[4]

Gold-containing compounds, exemplified by the first-generation gold-based drug auranofin, have been used in the treatment of rheumatoid arthritis (RA) for many years.[7] Recently, gold complexes have gained increasing attention in cancer therapy for their strong antiproliferation potency against cancer cells.[4,7−15] Studies of their mechanism indicated that some cysteine (Cys) and selenocysteine (Sec) -dependent enzymes might be their therapeutic targets. For example, auranofin was reported to strongly inhibit two Sec-containing enzymes, thioredoxin reductase (TrxR)[16] and glutathione peroxidase (GPx).[17,18] Auranofin was also shown to possess only modest inhibitory effect on glutathione reductase (GR), despite the similarity of GR and TrxR in their structure and function.[19] This was attributed to the higher affinity of auranofin to the Sec residue in selenoproteins than the cysteine in GR. However, this selectivity may have been much less expressed because of the widespread existence of serum albumin in vivo, which was found to react with auranofin by forming the putative Au(I)−S adduct.[20] In fact, many gold(I) compounds were discovered as binders of multiple S-donor proteins. It was reported that $[Au(d2pypp)_2]Cl$ can inhibit the activities of TrxR and its substrate, thioredoxin (Trx) by binding to the Cys pair at

Received: July 7, 2012

   dx.doi.org/10.1021/jm3009822 | J. Med. Chem. XXXX, XXX, XXX−XXX

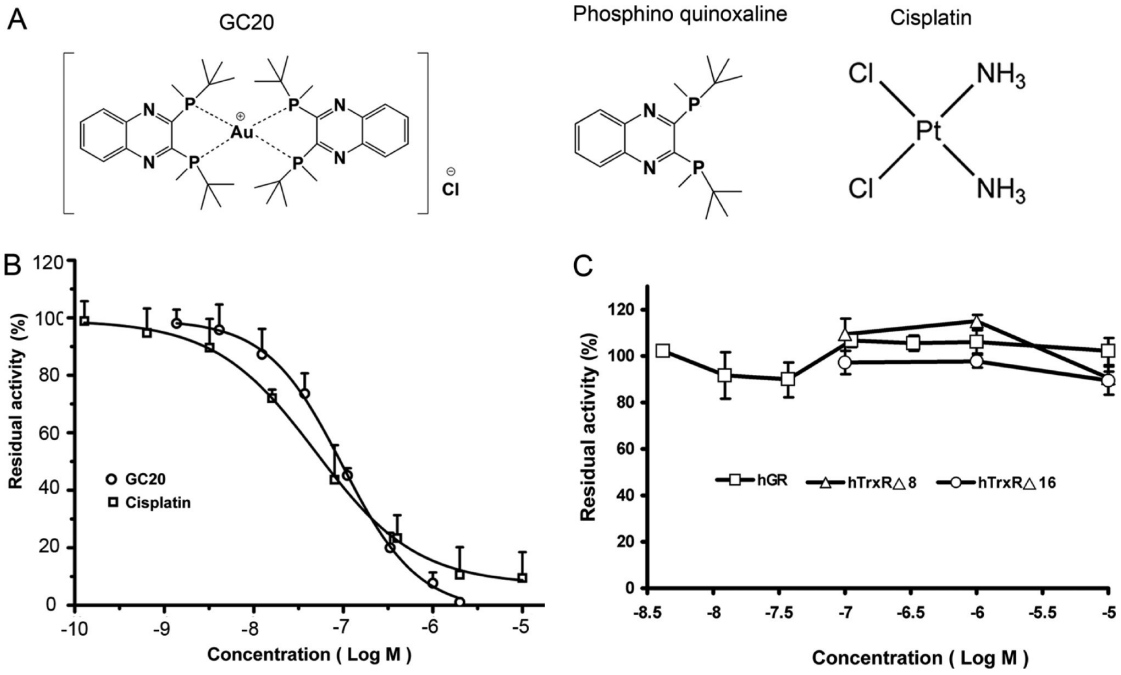

Figure 1. In vitro inhibition of TrxR activity by GC20 via binding to the C-terminal redox-active site. DTNB reduction assay was used to examine enzyme activities. (A) Structures of GC20, phosphinoquinoxaline, and cisplatin. (B) In vitro inhibition ability of GC20 and cisplatin. (C) Inhibitory ability of GC20 on the activity of hGR, determined with GSSG and insulin as substrates. Measurement of GC20 inhibition on hTrxRΔ8 and hTrxRΔ16 was performed via DTNB reduction assay.

the active site.[21] It was also shown that [1-phenyl-2,5-di(2-pyridyl)phosphole]AuCl can interact with GR in addition to TrxR. This was confirmed from the crystal structure of covalently modified GR with S−Au(I)−S coordination.[22] The high affinity of gold(I) compounds to thiols can lead to high toxicity and low efficacy in vivo due to the "off-target" effect. The quest for novel gold(I) compounds as therapeutically useful agents has received very limited success and is restricted only to animal studies. This is further borne out by the fact that no alternatives of gold(I)-containing compounds to cisplatin have been marketed to date.[7]

Among the targets mentioned above, TrxR has many advantages for the development of selective anticancer agents. TrxR plays important roles in many intracellular processes, such as regulation of redox metabolism, DNA synthesis, cell proliferation, signaling, and apoptosis.[23,24] There is ample evidence that TrxR is overexpressed and constitutively active in a variety of human tumors, and it is associated with tumor growth and angiogenesis.[23−27] Knockdown of TrxR in mouse lung carcinoma cells was reported to result in the recovery of both cell morphology and anchorage-independent growth properties similar to normal cells. When TrxR knockdown cells were injected into mice, tumor progression and metastases were dramatically reduced.[28] These results strongly suggest that TrxR is a promising anticancer target. More importantly, there is a Sec residue in the exposed and accessible C-terminal active site of TrxR. The pK_a value (∼5.3) of the functional Sec residue is significantly lower than that of Cys (pK_a = 8.4),[29] rendering a potentially higher reactivity for TrxR than the cysteine-dependent targets. It is therefore highly desirable to develop new anticancer agents by specifically targeting the Sec residue of TrxR.

Motivated by the great opportunities in the development of gold compounds as potential anticancer agents, we screened 16 new gold compounds on two human cancer cell lines. Among these compounds, a novel bis-chelated gold(I) diphosphine complex, GC20, was identified as the most promising one in terms of both its structure and activity. Specifically, we were able to show that GC20 has a strong growth inhibition property for a broad spectrum of cancer cell lines, including cisplatin-resistant ones. We report here our studies about the molecular target and the antiproliferation and anticancer potential of GC20. More importantly, we have found that GC20 shows a remarkable selectivity between cancer cells and normal cells as well as lower toxicity in animal models as compared to cisplatin. Our results suggest that GC20 has advantages over cisplatin and other metal-containing compounds in overcoming resistance, severe toxicity, and overreactivity and could potentially become a promising candidate for a new generation of gold(I)-based anticancer drugs.

RESULTS

Discovery of GC20. We originally performed antiproliferation screening of 16 in-house gold complexes against two human cancer cell lines: non-small-cell lung cancer (NSCLC) cells, NCI-H460, and gastric cancer cells, BGC-823 (Table S1 in Supporting Information). Among them, three compounds showed strong inhibition of proliferation of the two cancer cell lines. Subsequently we measured their anticancer potential and toxicity in vivo with sarcoma S180 xenograft-bearing Kunming mice. GC20, a bis-chelated gold(I) diphosphine compound (Figure 1A), showed less toxicity and strong anticancer potential compared with the other two compounds (Table S2 in Supporting Information). GC20 was shown to inhibit 50% of cell proliferation of both cell lines at a concentration of 0.5 μM and to inhibit 80.38% of tumor growth of sarcoma S180 xenografts in vivo at a dose of 8 mg/kg without loss of body weight at the same time.

GC20 Inhibits TrxR in Vitro by Binding to the C-Terminal Redox Site. To explore potential molecular targets for GC20, TrxR was chosen in our tests since it has been widely reported as the target of gold(I) compounds.[30,31] We tested the

dx.doi.org/10.1021/jm3009822 | J. Med. Chem. XXXX, XXX, XXX−XXX

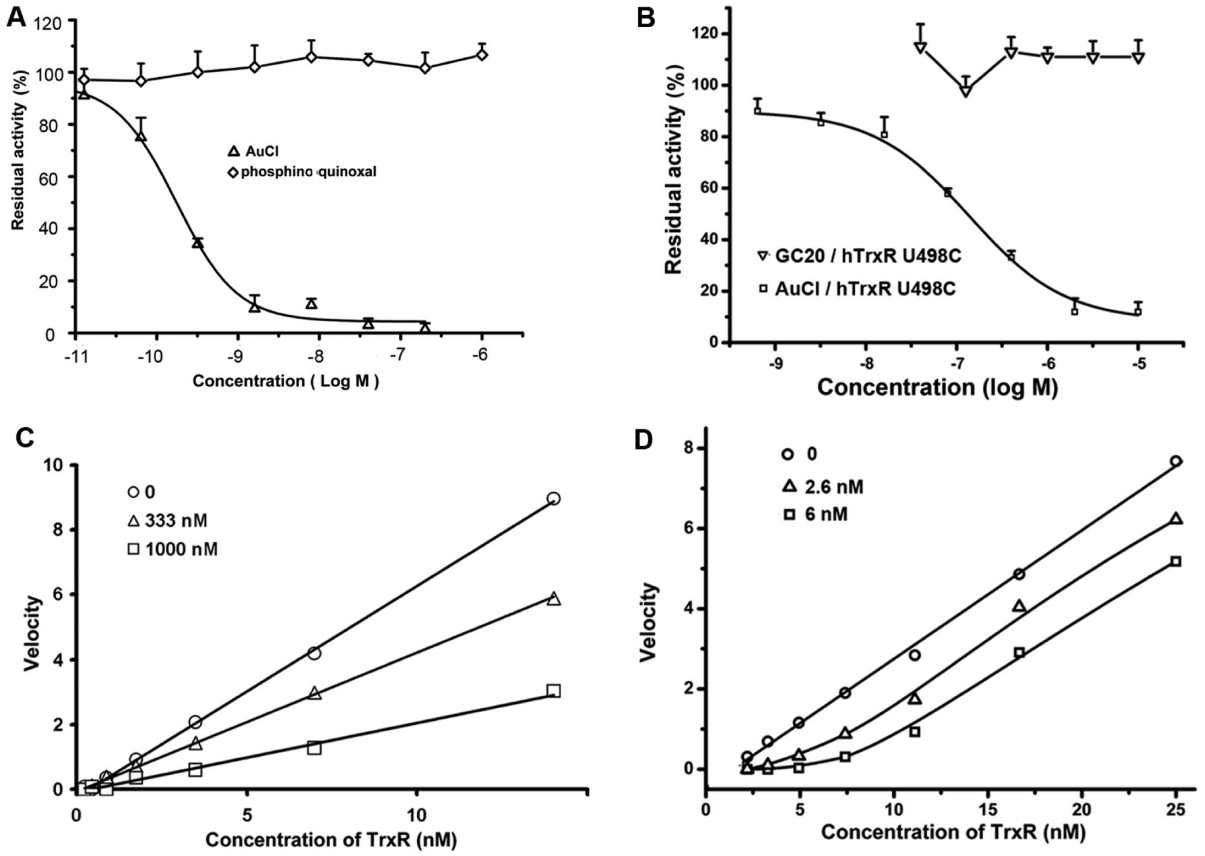

Figure 2. (A) Inhibition effects of free Au(I) in the form of AuCl and phosphinoquinoxaline ligand. (B) Inhibition potential of GC20 and AuCl on hTrxR U498C. (C, D) Ackermann–Potter plots of enzyme velocities in the presence of different concentrations of (C) GC20 and (D) AuCl. The product TNB increased over time in a linear manner, and the velocity was calculated as the slope (increase in absorbance per second).

enzymatic inhibition of TrxR by GC20 and cisplatin (Figure 1A). Inhibitory activity was examined by the 5,5′-dithiobis(2-nitrobenzoic acid) (DTNB) reduction assay. The in vitro IC_{50} of GC20 for TrxR is about 247.6 ± 42.1 nM, whereas the IC_{50} value of cisplatin is 74.9 ± 16.3 nM (Figure 1B). Previous studies have shown that TrxR has two redox-active sites, CVNCGC (59–64) in the N-terminus and GCUG (496–499) in the C-terminus.[32] To determine the potential binding site of GC20 in TrxR, we prepared two C-terminal mutants with the last 16 (hTrxRΔ16) or the last eight (hTrxRΔ8) amino acids truncated. We also tested hGR because some gold(I) compounds have been reported to covalently modify hGR with S–Au(I)–-S coordination.[22,33] GC20 showed no inhibition of either of the two C-terminal mutants or of hGR (Figure 1C), suggesting that its binding site is located at the C-terminal redox-active site in TrxR and also suggesting that its inhibitory mechanism is different than some reported Au(I) containing compounds.

To gain deeper insight into the GC20 inhibitory mechanism, we tested the inhibition activities of the coordinating ligand of GC20, {2,3-bis[*tert*-butyl(methyl)phosphino]quinoxaline}, and the free Au(I) in the form of AuCl. The phosphinoquinoxaline ligand alone has no inhibitory effect, while the free Au(I) shows extremely potent inhibition (IC_{50} = 1.7 ± 0.4 nM) (Figure 2A). Clearly, Au(I) is essential for the TrxR potency of GC20. Previous studies have shown that free Au(I) is not selective among different nucleophilic biomolecules.[34,35] Therefore, we constructed a mutant of TrxR (hTrxR U498C) with a mutation of Sec to Cys in the C-terminal active site. Interestingly, GC20 was inactive on the hTrxR U498C mutant even at high concentration of 10 μM, while free Au(I) showed strong inhibition with an IC_{50} value of 128.3 ± 15.7 nM (Figure 2B). Thus, it is not likely that GC20 could dissociate into free Au(I) in solution and subsequently inhibit TrxR.

GC20 Inhibits TrxR by a Reversible Mode of Action. We determined the catalytic velocities of TrxR in the presence of different concentrations of GC20 or AuCl, individually. From the Ackermann–Potter plot results, GC20 inhibits TrxR in a titration-dependent manner (Figure 2C), which is dramatically different than the tight binding mode of AuCl (Figure 2D). These results further indicate that GC20 is stable in solution and the inhibition of TrxR is attributed to the property of GC20 as a whole, rather than its ligand or the free Au(I).

Next, we wondered whether TrxR is reversibly inhibited by GC20. Therefore, we studied this inhibition mechanism using rapid dilution assay. It was shown that the incubation of TrxR with an irreversible inhibitor, curcumin,[36] resulted in formation of an enzyme–inhibitor complex that is resistant to dilution of the assay mixture (Figure 3A). In contrast, rapid dilution of the GC20/TrxR mixture leads to complete recovery of TrxR catalytic activity (Figure 3A), which suggests a reversible inhibition mechanism of GC20. Consistently, time-course experiments showed that the addition of GC20 resulted in an almost immediate inhibition, and no significant difference in the inhibition was observed during a nearly 2 h time course (Figure 3B).

GC20 Shows Selectivity between TrxR and Other Potential Targets. We have shown that GC20 can inhibit TrxR in vitro by selectively binding to Sec residue on the C-

dx.doi.org/10.1021/jm3009822 | J. Med. Chem. XXXX, XXX, XXX–XXX

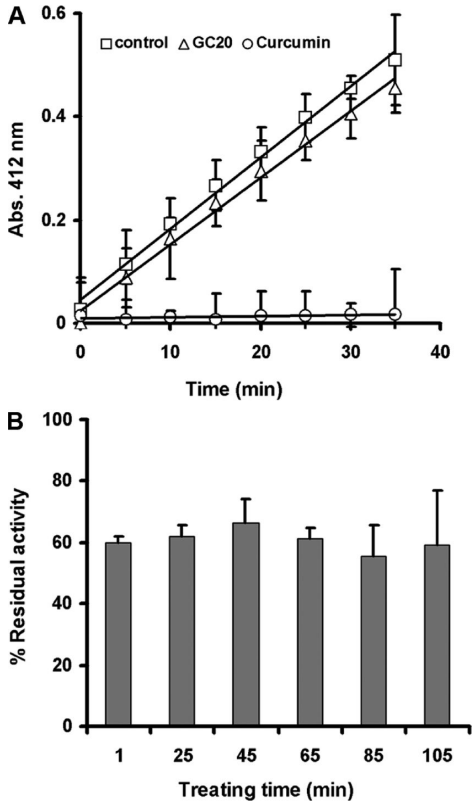

Figure 3. (A) Rapid dilution assays of TrxR in the presence of GC20 or curcumin (positive control). (B) Time course of TrxR inhibition by GC20 treatment. TrxR (3.5 nM) from rat liver was incubated with GC20 at 200 nM.

terminal active site. To confirm its ability to distinguish thiol and selenol groups, we also tested the effects of GC20 on Trx, since the Cys pair in the exposed active site can be readily targeted by gold(I) compounds such as $[Au(d2pypp)_2]Cl$.[21] As expected, GC20 did not show inhibition on Trx (Figure 4A), which confirms that GC20 interacts with Sec instead of Cys. In an attempt to further corroborate our findings, we examined the affinity of GC20 to another selenoprotein, human glutathione peroxidase (hGPx), reported to be inhibited by auranofin.[17] However, our result shows that GC20 has no effect on hGPx even at 50 μM (Figure 4B). The remarkable specificity of GC20 in targeting only TrxR but not hGPx can be attributed to the inaccessibility of the binding pocket of hGPx. Compared to hGPx, the active site of TrxR is much more accessible and can be easily approached by the structurally bulky and rigid GC20. These results indicate that both the superior reactivity of Sec and the highly exposed binding site contribute to the specificity of GC20 for TrxR.

GC20 Does Not Interact with Glutathione. Previous studies revealed that GSH is a major contributor to the resistance of cisplatin,[37,38] most likely as a result of an irreversible binding of the thiol functionality with platinum metal center. The level of GSH was shown to be much higher in cisplatin-resistant cancer cells. It conjugates with and hence consumes a majority of cisplatin in cytoplasm.[37,39] To evaluate its stability toward GSH, GC20 was incubated with various concentrations of GSH for 2 h and its UV absorption spectra were measured. It became immediately evident from the data (Figure 4C) that GC20 is remarkably stable even in the presence of a large excess (up to 14 equiv) of GSH. Furthermore, the UV spectra remain essentially unchanged after 24 h of incubation (Figure 4E). In comparison, absorbance of the GSH−Pt complex increases with both increasing concentration of GSH and incubation time (Figure 4D,F), which is consistent with previous reports that cisplatin can interact with GSH.[40]

GC20 Inhibits TrxR in Intact Cancer Cells. To determine whether GC20 would inhibit TrxR in intact cells, we treated human A549 tumor cell line with 2.0 μM GC20 for 6, 12, 24, and 48 h. Compared to the dimethyl sulfoxide (DMSO) control, GC20 was found to reduce the cellular enzymatic activity of TrxR by more than 40% after 6 h. Strikingly, cisplatin shows no inhibition at all compared to the phosphate-buffered saline (PBS) control despite its high inhibition activity in vitro. As expected, phosphinoquinoxaline ligand did not show any effect on cellular TrxR (Figure 5A). We also examined the effect of GC20 on the expression of TrxR by Western blot analysis. No significant changes were observed in the content of TrxR in cells treated by GC20 at different time points (Figure 5B). Clearly, the reduction of TrxR's activity is due to direct inhibition by GC20, rather than the downregulation of protein expression. It has been reported previously that 65−98% of the platinum in blood plasma was in protein-bound form after 1 day of administration.[1] The low efficacy of cisplatin on TrxR in cells that we observed here may result from its off-target binding with thiol-containing proteins such as bovine serum albumin (BSA) present in the complete culture medium. In addition, the antiproliferation potency of a variety of gold(I) compounds, including auranofin, is largely reduced by the fetal bovine serum (FBS) of culture medium in cell assays. This explanation was further supported by the observation that cisplatin shows strong TrxR inhibition in cell lysate, a FBS-free system (Figure 5C). All these results indicate that GC20 has the advantage of being stable in the cell culture system due to the absence of interaction, or a minimal if any interaction, with the thiol groups.

GC20 Shows Antiproliferation Potency on both Wild-Type and Cisplatin-Resistant Cancer Cells. The cellular activity of GC20 against a panel of different cancer cell lines was also assessed with 3-[4,5-dimethyl-2-thiazolyl]-2,5-diphenyl-2*H*-tetrazolium bromide (MTT) assay. With increasing concentration of GC20, cell viability was found to be significantly reduced after 48 h in the presence of FBS. GC20 showed broad growth inhibition on these cancer cells, with IC_{50} ranging from 0.1 to 2 μM. This makes GC20 quite different from other gold(I) compounds whose antiproliferation potency can be heavily reduced or even eliminated altogether by FBS.[41,42] It is shown that GC20 is more efficient than cisplatin, especially for the cisplatin-insensitive cell lines (Table 1). It is also evident that the phosphinoquinoxaline ligand of GC20 itself does not have any inhibitory effect on the cancer cells tested, including QGY-7701, HT-29, and BGC-823. In addition, the potential effect of GC20 on cisplatin-resistant cancer cells was also investigated, and our results show that GC20 can inhibit both cisplatin-resistant and wild-type cell lines (K111 and A549) with comparable potency (Table 1), while in comparison, cisplatin showed inhibition only in the two wild-type cell lines. In addition, the antiproliferation potency of GC20 in longer treatment time (3 and 5 days) was also measured with selected cancer cell lines. Similarly, GC20 inhibits cell proliferation even more strongly against these cancer cell lines (Table S3 in Supporting Information).

GC20 Induces Cell Cycle Arrest at G0/G1 Phase. We further studied the potential mechanistic pathway responsible for the strong antiproliferation potency of GC20. A549 cancer cells were treated with GC20 for 48 h at three concentrations around

dx.doi.org/10.1021/jm3009822 | J. Med. Chem. XXXX, XXX, XXX−XXX

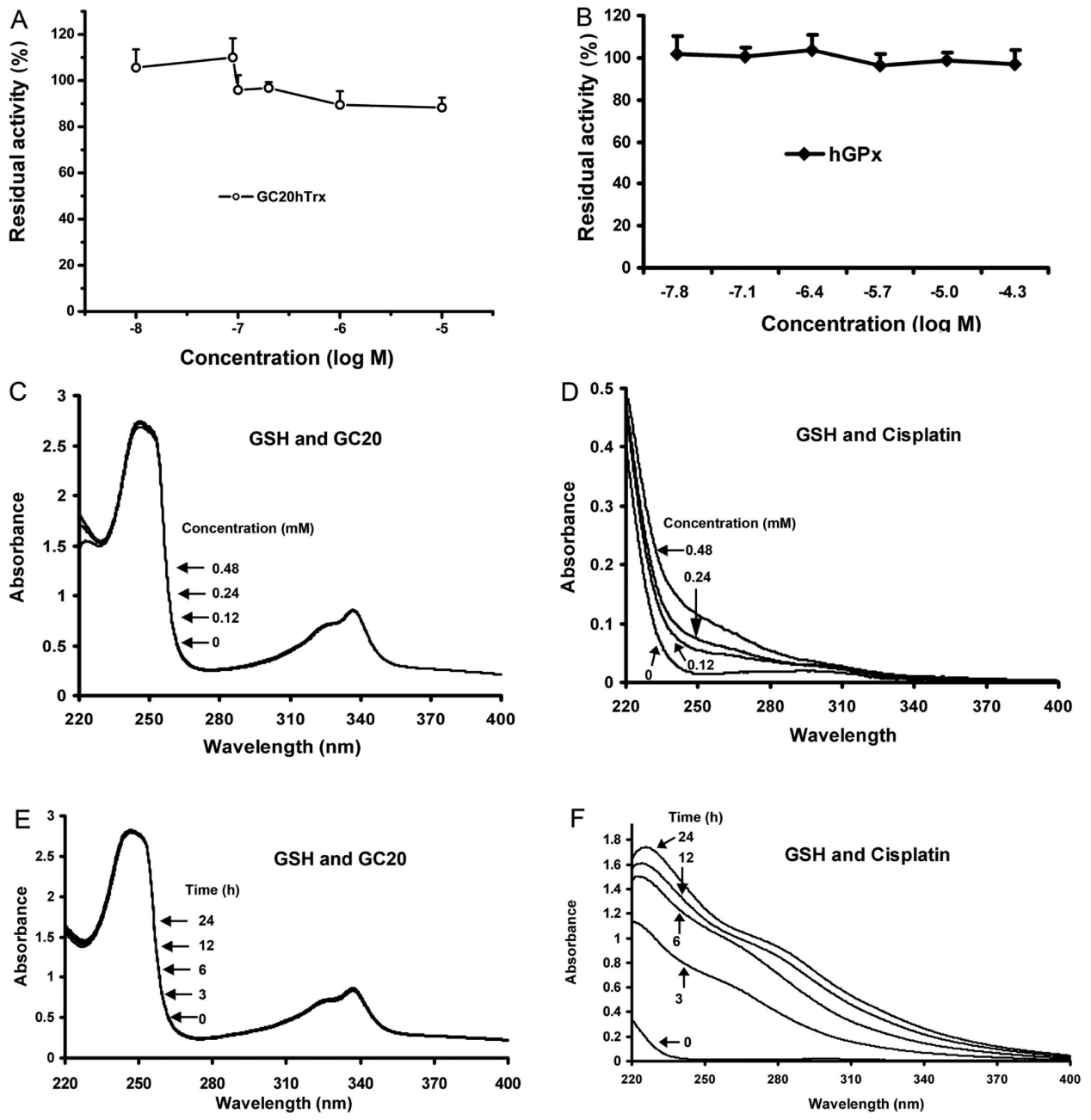

Figure 4. Selectivity of GC20 among other potential targets. (A) Inhibition of hTrx by GC20, evaluated with insulin turbidity assay. (B) Inhibitory ability of GC20 on hGPx, measured indirectly by a coupled reaction with GR. (C, D) Effect of different concentrations of GSH on the absorption spectra of (C) GC20 and (D) cisplatin. GC20 or cisplatin (0.035 mM) was incubated with varying concentrations of GSH in PBS at 37 °C for 2 h. The absorption spectrum of the sample was determined by scanning spectrophotometry over a wavelength range of 220−400 nm. (E, F) Effect of GSH on the absorption spectra of (E) GC20 and (F) cisplatin at different incubation times. GSH (3.33 mM) was incubated with 1.67 mM GC20 or cisplatin at 37 °C. A 10 μL aliquot of the reaction mixture was withdrawn at different time points and diluted with 490 μL of PBS. The absorption spectrum of the diluted sample was measured by scanning spectrophotometry over a wavelength range of 220−400 nm.

its IC_{50} value (0.25, 0.5, and 1 μM), and cell death was analyzed with propidium iodide (PI) staining (Figure S4 in Supporting Information). Very few stained cells were detected even at the high concentration of 1 μM, indicating that GC20 treatment at this concentration window does not induce significant cell death. Nevertheless, cell proliferation was found to be strongly inhibited by GC20 when compared to the DMSO control. We then investigated the cell cycle progression and found significant accumulation of cells at G0/G1 phase, with the reduction occurring at S phase (Figure 6A,B). Similar results were also observed in human renal cancer cells (SN12C) and human epithelial carcinoma cells (HeLa) after treatment with GC20 (Figure S5 in Supporting Information). These results further confirm the antiproliferation potency of GC20 in a broad spectrum of different cancer cell lines, most likely as a result of G1 arrest-induced cell growth inhibition. Previous studies have shown that cyclin D plays an important role in G1 to S phase progression and cyclin-dependent kinase (CDK) inhibitors contribute to G1 arrest, all of which function by regulating

dx.doi.org/10.1021/jm3009822 | J. Med. Chem. XXXX, XXX, XXX−XXX

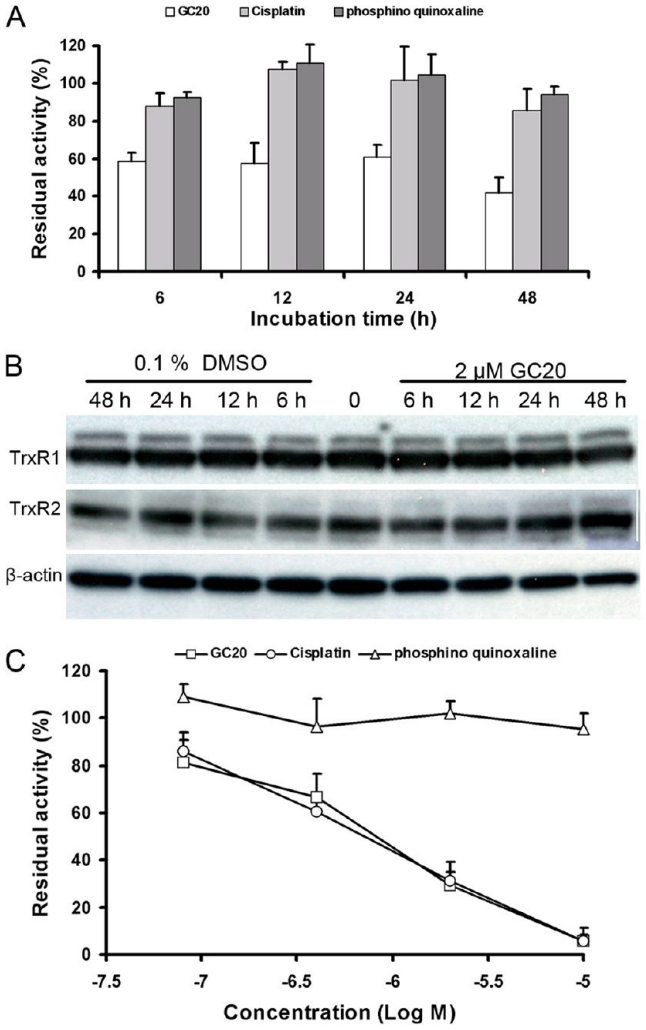

Figure 5. Inhibition of TrxR activity by GC20 in intact cancer cells. (A) TrxR activity inhibition in intact A549 cancer cells. Cells treated with 2.0 μM compounds for the indicated time intervals were collected and lysed before enzyme activity was determined. (B) Western blot results of TrxR expression in A549 tumor cells treated with 2 μM GC20 or 0.1% DMSO at different time points. (C) TrxR activity inhibition by GC20 and cisplatin in cell lysis. After A549 cells were collected and lysed, the inhibition activity of the two compounds in cell lysate was examined.

phosphorylation of downstream effector retinoblastoma (Rb) protein.[43]

These observations prompted us to examine the variance of G1-related targets by Western blot. Our result shows that 0.5 μM GC20 can induce significant reduction of cyclin D as well as the phosphorylation of Rb protein in A549 cancer cells at different time points (12, 24, and 48 h) while 0.1% DMSO has no effects on these targets (Figure 6C,D). However, no change was found in the expression of CDK inhibitors, including P15 INK4b, P16 INK4a, P21 Cip1, and P27 Kip1 (Figure S6 in Supporting Information). These results suggest that G1 arrest induced by GC20 results from the reduction of cyclin D expression and subsequent decrease in Rb phosphorylation rather than from inhibition of CDK activity by CDK inhibitors.

GC20 Exhibits High Selectivity between Cancer Cells and Normal Cells. The clinical utility of many anticancer agents possessing strong antiproliferation potency is hampered by the lack of their selectivity between cancer cells and normal cells. After we established the antiproliferation potency of GC20 against a broad spectrum of cancer cells, we subsequently studied its selectivity between NSCLC A549 cells and normal mouse embryonic fibroblasts (MEF) cells (gifts from Dr. Liang Chen, National Institute of Biology Sciences, Beijing, China). After treatment with GC20 for 48 h, A549 cells were found to be strongly inhibited (by more than 50%) at low concentrations (0.4−2 μM), whereas no effect was observed for MEF (Figure 7A). In contrast, cisplatin exhibited comparable effects on both cells at various concentrations. In other words, there was no difference in the response of A549 and MEF cells to cisplatin (Figure 7B). In addition, we measured the effects of GC20 against B-cells, T-cells, and peripheral blood mononuclear cells (PBMC) isolated from human peripheral blood in comparison with some human leukemia cell lines (Table S4 in Supporting Information). Clearly, human normal cells (PBMC, CD4+ T-cells, CD19+ B-cells) are resistant to the cytotoxic effects of GC20, which is in contrast to the effects seen in human leukemia cells. These results strongly support the high selectivity of GC20 in targeting cancer cells but not normal cells.

GC20 Shows Potential Anticancer Potency in Vivo with Low Toxicity. Encouraged by the remarkable selectivity of GC20 between cancer cells and normal cells as compared with cisplatin, we further investigated its potential as an anticancer agent by examining its activity and toxicity in animals. A549 tumor-bearing mice were treated with various doses of drugs or saline vehicle for 7 days. Nine days after withdrawal of the last treatment, tumor volume increased to 1850 ± 280 mm^3 in the saline control group. Remarkably, tumor volumes in the GC20 treatment group were limited to 360 ± 30, 510 ± 40, and 1040 ± 90 mm^3 at doses of 8, 4, and 2 mg/kg, respectively. The tumor growth inhibition ability of GC20 at 4 mg/kg is comparable to that of cisplatin at 2 mg/kg, for which the tumor volume increased to 530 ± 40 mm^3 (Figure 7C). The administration of GC20 was not shown to reduce the body weight of nude mice bearing A549 tumors even at doses as high as 8 mg/kg (Figure S7 in Supporting Information). Similar results were observed in several other xenografts, including murine hepatocellular carcinoma H22 cells, Lewis lung cancer cells, and LS174T human colon carcinoma cells (Figure S8 in Supporting Information).

To further establish the safety of GC20 in the mouse model, we examined its toxicity at extreme doses and long durations. Male and female ICR mice were selected and treated with a single dose of GC20 or cisplatin. The mortality in mice was monitored for 14 days after administration. The results (Table S5 in Supporting Information) indicated that GC20 has a LD_{50} of 42.31 ± 1.63 mg/kg for male mice and 41.04 ± 1.61 mg/kg for female mice, pointing to a much lower toxicity than that of cisplatin (LD_{50} = 12.27 ± 2.25 mg/kg for male, LD_{50} = 11.27 ± 2.44 mg/kg for female). In separate experiments, Sprague-Dawley rats were injected daily with either GC20 at doses of 2, 4, and 8 mg/kg or cisplatin at 1 and 2 mg/kg for 28 days, and the mortalities were measured. The results show that no rat died in the GC20-treated group and there was little loss of body weight. In contrast, all rats treated with 2 mg/kg cisplatin died within 7−10 days. Note that at the dose of 1 mg/kg for cisplatin, eight out of 10 rats died in 28 days (survival rate = 20%) (Figure 8A). Many anticancer agents cause hematologic toxicity. Thus, we also examined the changes of the levels of red and white blood cells (Figure 8B,C) as well as leukocytes and granulocytes (Table S6 in Supporting Information) in the peripheral blood of SD rats for 28 days after treatment with GC20. No statistically significant changes occur after GC20 treatment ($p > 0.05$).

dx.doi.org/10.1021/jm3009822 | J. Med. Chem. XXXX, XXX, XXX−XXX

Table 1. Antiproliferation Potency of GC20 against Various Cancer Cell Lines and Cisplatin-Resistant Cell Lines

		IC_{50} (mean ± SD, μM)		
cell line	cell type	GC20	cisplatin	phosphinoquinoxaline
NCI-H460	non-small-cell lung cancer	0.3 ± 0.3	8.4 ± 3.1	
A549	non-small-cell lung cancer	0.4 ± 0.4	7.9 ± 1.9	
HepG2	liver cancer	1.2 ± 0.4	18.7 ± 13.3	
QGY-7701	liver cancer	0.3 ± 0.2	9.1 ± 4.6	>300.0
Hep-3B	liver cancer	0.7 ± 0.2	7.6 ± 0.5	
HT-29	colon cancer	0.3 ± 0.2	35.6 ± 12.1	>300.0
SW620	colon cancer	0.3 ± 0.2	74.7 ± 0.1	
BGC-823	gastric adenocarcinoma	0.6 ± 0.7	5.5 ± 3.9	>300.0
SGC-7901	gastric adenocarcinoma	0.8 ± 0.2	2.5 ± 0.9	
SK-OV-3	ovarian cancer	0.5 ± 0.50	2.1 ± 21.4	
TC-1	ovarian cancer	0.7 ± 0.2	4.8 ± 4.5	
MCF7	breast cancer	0.4 ± 0.2	12.7 ± 8.8	
MDA-MB-231	breast cancer	9.2 ± 0.6	44.6 ± 0.2	
A375	melanoma	1.6 ± 0.1	4.6 ± 2.4	
K111	melanoma	1.8 ± 0.7	15.5 ± 13.8	
K-562	leukemia	0.3 ± 0.2	9.0 ± 7.4	
L1210	leukemia	0.3 ± 0.4	2.4 ± 0.7	
KB	nasopharyngeal epidermoid	1.0 ± 0.7	4.9 ± 1.6	
K111 (cisplatin-resistant)	melanoma	0.1 ± 0.3	237.2 ± 30.0	
A549 (cisplatin-resistant)	non-small-cell lung cancer	0.11 ± 0.03	>333.3	

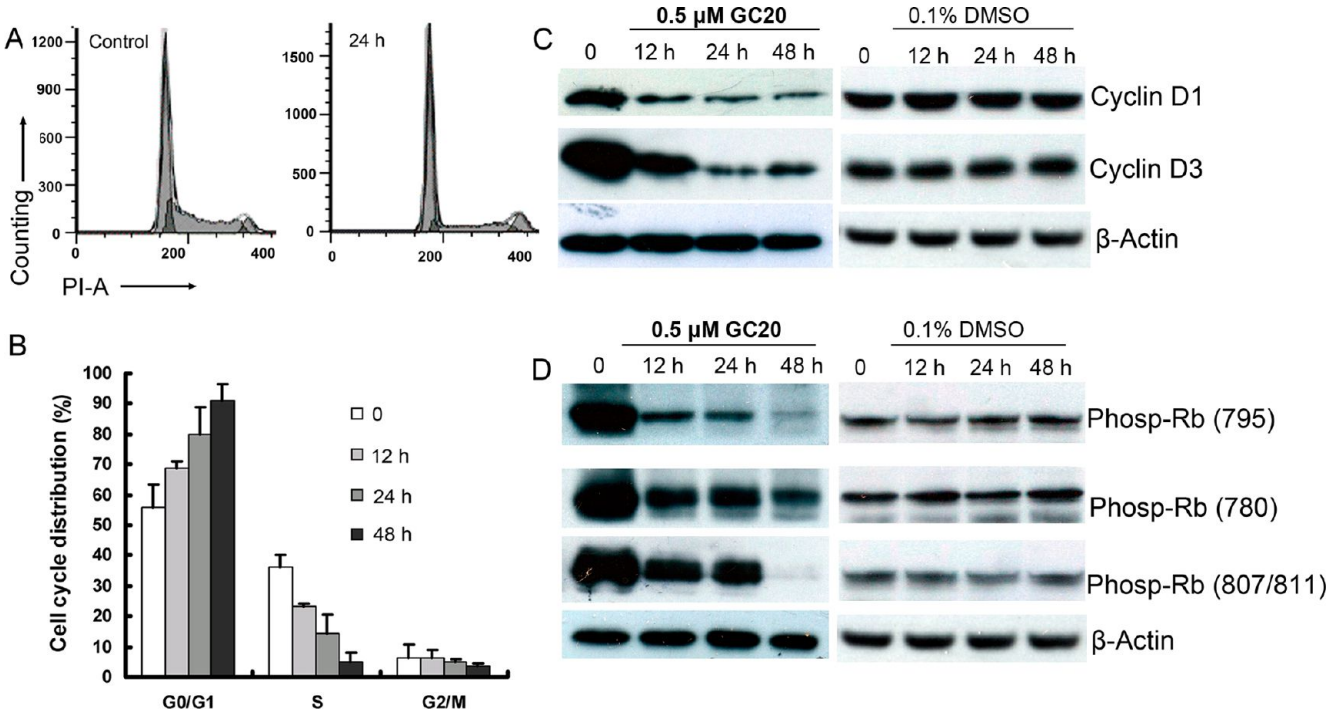

Figure 6. Cell cycle arrest at G0/G1 phase with reduction in cyclin D expression and Rb protein phosphorylation induced by GC20. A549 cells were treated with 0.5 μM GC20 for 12, 24, and 48 h, and the cell cycle distribution was measured by flow cytometry. Protein expression and phosphorylation levels were analyzed by Western blots. (A) Representative plots of one time point in one set of triplicate experiments. G0/G1, S, and G2/M of the cell cycle were sorted on the basis of DNA content after being stained with PI. (B) Bar graph of cell distributions. Means and SD were calculated from triplicate independent experiments. (C, D) Expression of cyclins D1 and D3 and the phosphorylation level of Rb protein. Samples were probed with anti-β-actin as loading control.

DISCUSSION AND CONCLUSION

Despite its historical success as a clinically useful chemotherapy drug, cisplatin suffers from some major drawbacks such as acquired resistance in long-term treatment, severe toxicity, and occurrence of cisplatin-insensitive tumors, just to name a few. Among them, enhanced GSH level and increased DNA repair were considered to contribute to the resistance.[1,40] Extensive study has shown in the past that many gold-containing compounds are reactive toward Cys-containing proteins,[20] resulting in reduced efficacy and severe toxicity. Thus, the development of novel gold compounds with synergistic reactivity and selectivity is highly desirable.

dx.doi.org/10.1021/jm3009822 | J. Med. Chem. XXXX, XXX, XXX−XXX

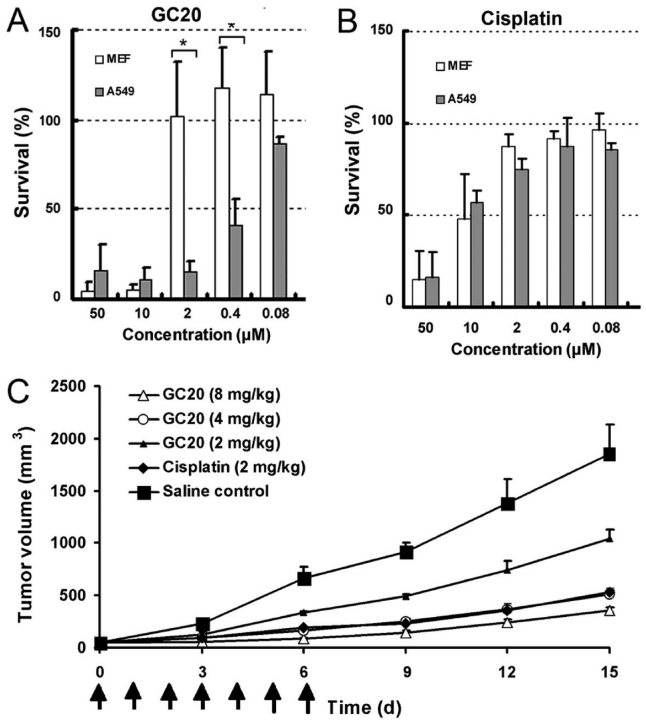

Figure 7. Selectivity of GC20 between normal cells and cancer cells in vitro and antitumor ability in vivo. (A) Antiproliferation potential of GC20 on MEF and A549. (B) Antiproliferation potential of cisplatin on MEF and A549. A549 or MEF cells were seeded into the 96-well plate and different concentrations of GC20 or cisplatin were then added to the cells after 12 h. The cell viability was measured with MTT assay after the cells were treated with cisplatin for 48 h. (C) Inhibitory ability of GC20 on the growth of A549 tumor on nude mice. After establishment of solid tumor, the mice were randomized and treated with saline control, cisplatin, or GC20 once daily intravenously at the indicated doses for 7 days (indicated with arrows); the tumor volume was calculated according to the width and length of tumors every 3 days during the whole process.

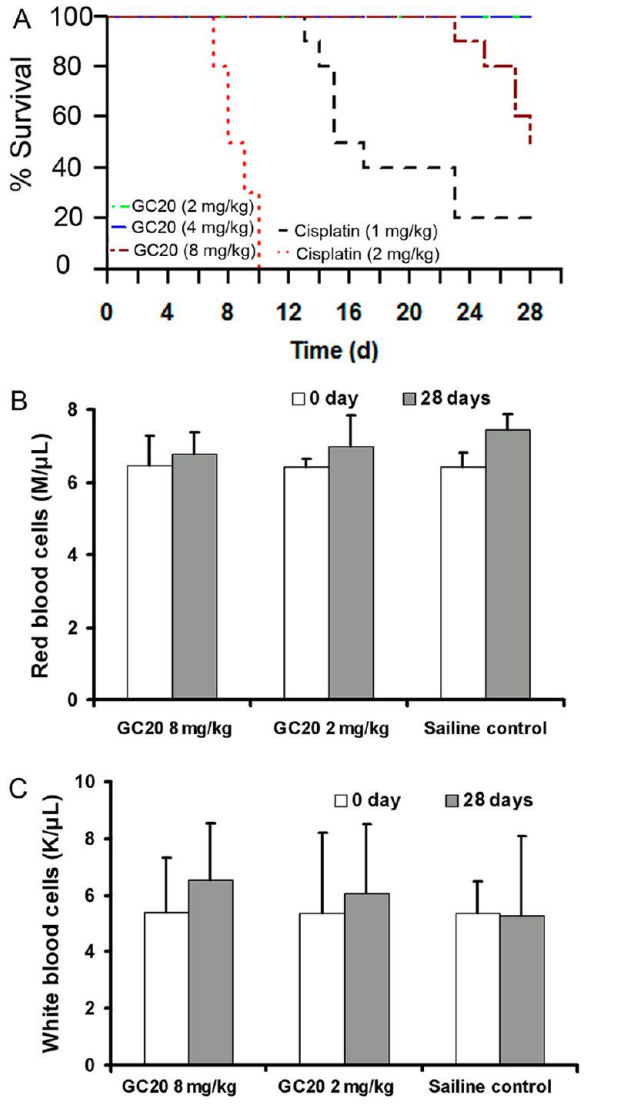

Figure 8. (A) Kaplan–Meyer plot of survival of SD rats treated with GC20 and cisplatin. (B, C) Numbers of (B) red blood cells (RBC) (M/μL) and (C) white blood cells (WBC) (K/μL) in the peripheral blood of SD rats were measured before and after the treatment with GC20 for 28 days (n = 10/group).

In this study, we have discovered that a novel gold(I) compound, GC20, can selectively inhibit TrxR both in vitro and in cancer cells, without reacting with other thiol- or selenol-dependent targets, including GR, Trx, and GPx as well as TrxR functional mutants and deletions (hTrxRU498C, hTrxRΔ8, and hTrxRΔ16,). In addition, we observed that GSH does not react with GC20, and the antiproliferation potency of GC20 is not impeded by the presence of FBS in medium. According to previous reports, GSH is considered to be a major contributor to cisplatin resistance.[40] Serum albumin was shown to react with many well-studied gold(I) compounds and to reduce their efficacy in vivo.[20,41,42] The high reactivity toward thiols can also lead to "off-target" binding or even severe side effects. Our findings show that GC20 has the advantage of being highly selective while maintaining a balanced and synergistic reactivity.

Further evaluation of its cellular performance revealed that GC20 can strongly inhibit the proliferation of a broad spectrum of cancer cell lines, including NSCLC, liver, colon, gastric, ovarian, breast, and melanoma cancers as well as leukemia, with IC_{50} ranging from 0.1 to 2 μM. Some of these cell lines were shown to be insensitive to cisplatin, with IC_{50} higher than 20 μM. Our results strongly suggest that GC20 may provide an alternative way for the treatment of cisplatin-insensitive cancers. For example, GC20 was shown to have potent inhibition of two cisplatin-resistant cell lines. Specifically, GC20 was found to inhibit both K111 and A549 resistant cells by 50% at concentrations as low as 0.1 μM, whereas their IC_{50} with cisplatin is >200 μM. The positive performance that we observed with GC20 helps further strengthen the notion that GC20 may have the potential to be a useful therapeutic agent in the treatment of a broad range of tumors.

In our study on its molecular mechanism, we have found that 0.5 μM GC20 could induce significant cell cycle arrest of A549 tumor cells by more than 20% in G1 phase after 24 h. Western blot further revealed consistent variance in G1-related targets, including reduction of cyclin D expression and decrease of Rb protein phosphorylation. Previous studies have indicated that the knockdown of TrxR in cancer cells may induce defects in G1/S transition,[44] and recovery was noticed in both cell morphology and anchorage-independent growth property close to normal cells.[28] Similarly, Trx knockdown can result in significant G1 arrest with reduced cyclin D expression in A549 cancer cells, which is consistent with our observations.[45] Several possible mechanisms that might be responsible for the TrxR inhibition-

dx.doi.org/10.1021/jm3009822 | J. Med. Chem. XXXX, XXX, XXX–XXX

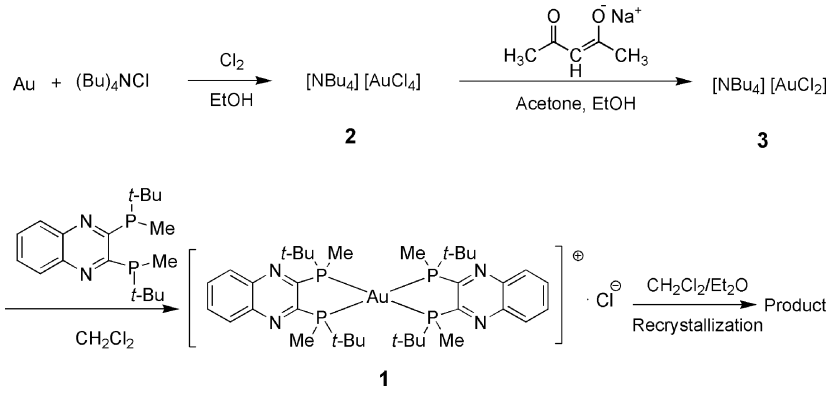

Figure 9. Synthetic route to GC20.

induced antiproliferation potency have been proposed. In the most prevailing mechanism, it was believed that TrxR inhibition could alter the permeability of mitochondrial membrane and induce mitochondria swelling and loss of membrane potential.[46−48] According to a second mechanism, inhibition of TrxR could increase the level of reactive oxygen species (ROS) and lead to the overactivation of mitogen-activated protein kinase (MAPK) pathway.[49] In a third mechanism that has been proposed, inhibition of TrxR was believed to induce the constitutive activation of apoptosis signal-regulating kinase (ASK1), which can be inhibited by Trx only in the reduced state.[50] These processes can all induce cell cycle arrest and/or cell death.[31] At this time, a clear distinction among these mechanisms with regard to the action of GC20 is still premature, based on the above-mentioned observation, and our ongoing research is directed toward this goal.

We further examined the toxicity of GC20 both in cells and in animals. In cells, GC20 was found to possess strong inhibition against A549 but not MEF at concentrations as low as 0.4 μM, whereas cisplatin did not show any effects on A549 at low concentrations. At high concentrations (10 μM), cisplatin inhibited both A549 and MEF cells by 50%. In addition, human leukemic and lymphoblast cells were shown to be much more sensitive to GC20 treatment than human normal cells isolated from peripheral blood. In mouse xenograft models, GC20 has comparable antitumor potential with that of cisplatin, yet it has a better safety profile than cisplatin, either at extreme doses (GC20, LD_{50} = 42.31 ± 1.63 mg/kg for male and 41.04 ± 1.61 mg/kg for female; cisplatin, LD_{50} = 12.27 ± 2.25 mg/kg for male and 11.27 ± 2.44 mg/kg for female) or in long duration experiments (GC20, survival rate = 100% for as high as 4 mg/kg; cisplatin, survival rate = 20% for as low as 1 mg/kg). Furthermore, no obvious hematologic toxicity was observed in animals after GC20 treatment for 28 days, which is consistent with our safety studies at the cellular level. These results all strongly suggest that GC20 is less toxic than cisplatin but has very comparable efficacy in vivo. When these results are taken together, GC20 has the potential to become a promising drug candidate in cancer therapy.

EXPERIMENTAL SECTION

Synthesis of GC20. The synthesis of GC20 (Figure 9) began with gold powder of purity greater than 99.99% as starting material. Both gold powder (30.0 g, 0.15 mol) and $(Bu)_4NCl$ (63.5 g, 0.23 mol) were added in ethanol (1600 mL) simultaneously in the presence of chlorine with stirring at room temperature (RT). Once the oxidation was complete, the reaction mixture was cooled overnight and followed with filtration and drying to give product **2** as orange-colored needlelike crystals (75.2 g) with yield of 85%. Before the synthesis of **3**, we prepared the reactant acetylacetone sodium. Acetylacetone (309 mL, 3 mol) was slowly added dropwise to a solution of NaOH (80 g, 2 mol) in methanol/water (4:1; 500 mL). During the whole process, the mixture was stirred at RT so that the temperature of the reaction system remained constant. Once the reaction was finished, the products were washed three times with ice-cooled methanol after filtration in vacuum and then placed in a vacuum drying oven to give the product as a white solid (191.9 g) in 94% yield. The reactant acetylacetone sodium (7.9 g, 0.065 mol) was added and dissolved in ethanol (180 mL) with reflux in an oil bath. Once the desolvation was complete, the ethanol solution of acetylacetonate sodium was transferred to a 250 mL dropping funnel and slowly added to **2** (30.0 g, 0.05 mol) in acetone solution (180 mL) dropwise. The reaction was stopped after reflux for 12 h in the oil bath. The mixture was filtered to remove undissolved substance and was concentrated to get a white solid, which was further recrystallized with ethanol to give white needlelike crystals **3** (24.5 g), in 93% yield. Compound **3** (20.0 g, 0.039 mol) was added and dissolved in dichloromethane (100 mL). On the other hand, Quinox P (26.3 g, 0.078 mol) was also dissolved in dichloromethane (100 mL) and transferred to a 200 mL dropping funnel to be added to the solution of **3** dropwise. The reaction proceeded for 12 h at RT, and then the mixture was extracted with NaCl solution (0.9%, 160 mL) twice. After drying with anhydrous sodium sulfate as well as filtration and concentration, 40.8 g of **1** as a dark red solid was obtained. The pure product **1** was obtained from recrystallization with mixed organic solvent in 84% yield. The purity of target compound was determined by HPLC (>99% purity), MS spectra were recorded on a Micromass Q-Tof micro, and ^{1}H NMR was recorded on a Varian INOVA-400 NMR system (Figures S1−S3 in Supporting Information).

Cells and Animals. All cancer cell lines were obtained from the Shanghai Institute of Biochemistry and Cell Biology (SIBCB) and cultured in RPMI 1640 medium (Gibco) containing 10% fetal bovine serum (FBS) at 37 °C in a humidified incubator with 5% CO_2. Nude and ICR mice and Sprague-Dawley[51] rats were purchased from Shanghai Laboratory Animal Center (SLAC, Shanghai, China). Animals were housed under standard laboratory conditions with free access to food and water.

Expression and Purification of hTrxRU498C, hTrxRΔ8, and hTrxRΔ16. The hTrxRU498C construct in pET28a(+) is a gift from Katja Becker, Interdisciplinary Research Center, Justus Liebig University, Germany. The hTrxR gene lacking the last 24 or 48 bp was cloned into the pET28a(+) expression vector to produce hTrxR truncated mutants hTrxRΔ8 and hTrxRΔ16. Protein expression and purification were performed as described previously.[52] The purity of the product was checked with sodium dodecyl sulfate−polyacrylamide gel electrophoresis (SDS−PAGE).

In Vitro Enzymatic Activity Assays. For inhibition of rat liver TrxR (Sigma−Aldrich), hTrxRU498C, hTrxRΔ8, and hTrxRΔ16, the 5,5′-dithiobis(2-nitrobenzoic acid) (DTNB) reduction assay was performed according to manufacturer's instructions (Sigma−Aldrich product information sheet T9698). Typical reaction mixture (200 μL)

dx.doi.org/10.1021/jm3009822 | J. Med. Chem. XXXX, XXX, XXX−XXX

consists of 3.5 nM rat liver TrxR (or 140 nM TrxRU498C, or 200 nM hTrxRΔ8, or 200 nM hTrxRΔ16). The rate of formation for 5-thionitrobenzol (TNB) was determined by measuring the increase in absorption (Δ412/min) with a Beckman Coulter paradigm detection platform. The enzyme activities were calculated as the slopes (increase in absorbance per second). The IC_{50} values were calculated as the concentration of compound that decreased the enzymatic activity of the untreated control by 50%.

For inhibition studies on hGR, the GSSG reduction assay was carried out according to the manufacturer's instructions (Sigma–Aldrich product information sheet GRSA). Typically, 70 nM hGR (Sigma–Aldrich) was used in the 200 μL reaction cocktail. Measurement of increase of TNB and calculation of the enzymatic activity were done in the same way as for the TrxR assay.

For inhibition studies on hGPx, a commercially available kit (glutathione peroxidase activity kit; Cayman Chemical Co.) was used as directed in the manual. The activity of hGPx was measured indirectly by the coupled reaction with GR. The 200 μL reaction cocktail contains 30 ng of hGPx (Sigma–Aldrich). The activity of hGPx was calculated by measuring the decrease in absorbance at 340 nm.

For inhibition studies on hTrx, the insulin turbidity assay was performed as described previously.[53] Briefly, 0.47 μM hTrx (Sigma–Aldrich) was mixed with the reaction cocktail (100 mM phosphate buffer, pH 7.0, 0.15 mM bovine insulin, 1 mM ethylenediaminetetraacetic acid (EDTA), and 0.1% Triton X-100). The reaction was initiated by adding 330 μM dithiothreitol (DTT) to the mixture. The turbidity of the solution was then continuously monitored at 650 nm.

Rapid Dilution Assay. Rapid dilution assay was performed as described previously.[54,55] Briefly, 500 nM TrxR is incubated with 2.5 μM GC20 or 50 μM curcumin for 30 min. After 100-fold rapid dilution of the mixture, enzyme activity was measured as an increase in absorbance at 412 nm for 35 min.

UV Spectral Analysis. To determine the interaction between GSH and GC20, a well-established UV absorbance spectrum analysis was performed.[40] Briefly, compounds were incubated with different concentrations of GSH for 2 h or incubated with GSH for different time intervals at 37 °C. The absorption spectrum was recorded by wavelength scanning over the range 220–400 nm on a UV–visible spectrophotometer (Shimadzu UV-2450).

Cellular TrxR Activity Inhibition Assay. A549 cells were treated with 2.0 μM compounds in complete Dulbecco's modified Eagle's medium (DMEM) (Invitrogen) for 6, 12, 24, or 48 h. The cells were washed with PBS three times and lysed with mammalian cell lysis/extraction reagent (Sigma–Aldrich) according to the instruction manual. The protein concentration in the supernatant was determined by use of Bradford reagent (Sigma–Aldrich). Examination and calculation of TrxR activity in cells were done in the same way as for the in vitro assays.

Establishment of Cisplatin-Resistant Cell Lines. Cisplatin-resistant sublines from K111 and A549 were established by continuous exposure to cisplatin, as previously described.[56] Both cell lines were exposed to stepwise increases in concentrations of cisplatin, beginning with 0.7 μM and doubly increased to 180 μM after the cells had regained their exponential growth rate.

Cellular Antiproliferation Assay. Cellular antiproliferative assays were carried out by the MTT (3-[4,5-dimethyl-2-thiazolyl]-2,5-diphenyl-2*H*-tetrazolium bromide) method as previously described.[57] Briefly, cells (100 μL) were incubated with various concentrations of compounds in a 96-well plate for 48 h at 37 °C. Then 10 μL of MTT (5 mg/mL) solution was added to each well. After further incubation at 37 °C for 4 h, formazan formed from MTT was extracted by adding 100 μL of DMSO for 12 h. Absorbance at 492 nm was then determined on a microplate reader, and the IC_{50} values were calculated from the inhibition ratios.

Cell Cycle Distribution Analysis. The effect of GC20 on cell cycle distribution was measured with flow cytometry. A549 cells were incubated in complete culture medium with 0.5 μM GC20 for 12, 24, and 48 h. Cells were harvested and fixed with 70% ethanol overnight at −20 °C. Then cellular DNA was stained with 100 mg/mL propidium iodide (PI) and 100 mg/mL RNase A in PBS. Flow cytometry was performed to determine the cell cycle distribution on a FACSCalibur flow cytometer (Becton Dickinson). Data were analyzed with FlowJo software (Tree Star, Ashland, OR).

Antibodies and Immunoblotting. Anti-β-actin was purchased from Abcam. All other primary antibodies were from Cell Signaling Technology. Cells were harvested and lysed with mammalian cell lysis/extraction reagent (Sigma–Aldrich). The protein concentration was determined with Bradford reagent (Sigma–Aldrich) according to manufacturer's instructions. Western blot analysis was conducted according to standard procedures.

A549 Tumor Xenograft Studies. Subcutaneous flank tumors were established by inoculating small A549 tumor pieces into female nude mice. Tumor volumes (cubic millimeters) were calculated from measurement of the length (L) and width (W) of tumors by the formula $0.5 \times L \times W^2$. When flank tumors had grown to about 50 mm^3, the mice were treated once daily intravenously with GC20 (2, 4, and 8 mg/kg), cisplatin (2 mg/kg), or saline vehicle for 7 days. During the whole process, we examined the volume of tumor every 3 days. The mice were sacrificed and tumors were dissected and weighed 9 days after withdrawal of drug treatment.

Animal Toxicity Studies. ICR mice (18–20 g) were used to evaluate the toxicity of GC20. The compounds tested were administered in single intravenous doses (for GC20, 55.0, 46.8, 39.7, 33.8, and 28.7 mg/kg; for cisplatin, 20.0, 16.0, 12.8, 10.2, and 8.2 mg/kg) with saline vehicle as control. Each concentration was applied to 10 female mice and 10 male mice. Changes in the appearance, behavior, and mortality in mice were monitored for 14 days after administration. The median lethal dose (LD_{50}) values were determined by the Bliss method. In addition, Sprague-Dawley rats (120–140 g) were injected intravenously with GC20 (2, 4, and 8 mg/kg) and cisplatin (1 and 2 mg/kg) daily for 28 days to measure the long-term toxicity. The mortality of rats was monitored and recorded daily.

Measurement of Hematologic Effects. Following treatment of GC20 at doses of 8 and 2 mg/kg for 28 days, the numbers of white blood cells (WBC) and red blood cells (RBC) as well as leukocytes and granulocytes were measured with a multispecies hematology system (HEMAVET 950, Drew Scientific Inc.).

Data Analysis and Statistics. All experiments were performed three times with 10 samples/group. All results were derived from at least three independent experiments. Data are shown as mean values ± SD. Statistical analyses were performed by use of Student's *t* test.

■ ASSOCIATED CONTENT

Supporting Information

Eight figures and six tables showing HPLC, MS, and NMR spectral data of GC20, PI fluorescence and cell morphology of GC20-treated A549 cells, GC20-induced G1 cell cycle arrest, Western blot results of CDK inhibitors in GC20-treated A549 cells, antitumor ability of GC20 on various xenografts, antiproliferative activity of screened gold-containing compounds and anticancer potential of selected compounds, IC_{50} of GC20 against different cancer cell lines at different treatment times, IC_{50} of GC20 against human leukemic and lymphoblast cells and normal cells isolated from peripheral blood, and acute toxicity. This material is available free of charge via the Internet at http://pubs.acs.org.

■ AUTHOR INFORMATION

Corresponding Author

*(N.H.) phone 86-10-80720645, fax 86-10-80720813, e-mail huangniu@nibs.ac.cn; (Q.L.) phone 86-21-65179533, fax 86-21-65449361, e-mail liuquanhai_lqh@163.com.

Author Contributions

∥These authors contributed equally to this work.

Notes

The authors declare no competing financial interest.

dx.doi.org/10.1021/jm3009822 | *J. Med. Chem.* XXXX, XXX, XXX–XXX

■ ACKNOWLEDGMENTS

We thank Professor Katja Becker (Interdisciplinary Research Center, Justus Liebig University, Germany) for generously providing us the hTrxR construct. We also thank Dr. Liang Chen (National Institute of Biology Sciences, Beijing, China) for providing MEF cells. We thank Nippon Chemical Industrial Co., Ltd., for providing the compound sample of GC20. Financial support from the Chinese Ministry of Science and Technology "973" Grant 2011CB812402 (to N.H.), the Key New Drug Creation and Manufacturing Program 2009ZX09120-055 and Shanghai Committee of Science and Technology 08410703600 (to Q.H.L.) is gratefully acknowledged.

■ ABBREVIATIONS USED

RA, rheumatoid arthritis; TrxR, thioredoxin reductase; GPx, glutathione peroxidase; GR, glutathione reductase; NSCLC, non-small-cell lung cancer; GSH, glutathione; BSA, bovine serum albumin; RB, retinoblastoma; MEF, mouse embryonic fibroblasts; ROS, reactive oxygen species; MAPK, mitogen-activated protein kinase; ASK, apoptosis signal-regulating kinase; DTNB, 5,5′-dithiobis(2-nitrobenzoic acid); TNB, 5-thionitrobenzol; RBC, red blood cells; WBC, white blood cells

■ REFERENCES

(1) Alderden, R. A.; Hall, M. D.; Hambley, T. W. The discovery and development of cisplatin. *J. Chem. Educ.* **2006**, *83*, 728−734.
(2) Antman, K. H. Introduction: the history of arsenic trioxide in cancer therapy. *Oncologist* **2001**, *6* (Suppl. 2), 1−2.
(3) Lebwohl, D.; Canetta, R. Clinical development of platinum complexes in cancer therapy: an historical perspective and an update. *Eur. J. Cancer* **1998**, *34*, 1522−1534.
(4) Bruijnincx, P. C.; Sadler, P. J. New trends for metal complexes with anticancer activity. *Curr. Opin. Chem. Biol.* **2008**, *12*, 197−206.
(5) Giaccone, G. Clinical perspectives on platinum resistance. *Drugs* **2000**, *59* (Suppl. 4), 9−17.
(6) Kelland, L. R. Preclinical perspectives on platinum resistance. *Drugs* **2000**, *59* (Suppl. 4), 1−8.
(7) Nobili, S.; Mini, E.; Landini, I.; Gabbiani, C.; Casini, A.; Messori, L. Gold compounds as anticancer agents: chemistry, cellular pharmacology, and preclinical studies. *Med. Res. Rev.* **2010**, *30*, 550−580.
(8) Gandin, V.; Fernandes, A. P.; Rigobello, M. P.; Dani, B.; Sorrentino, F.; Tisato, F.; Bjornstedt, M.; Bindoli, A.; Sturaro, A.; Rella, R.; Marzano, C. Cancer cell death induced by phosphine gold(I) compounds targeting thioredoxin reductase. *Biochem. Pharmacol.* **2010**, *79*, 90−101.
(9) Berners-Price, S. J.; Fau-Filipovska, A.; Filipovska, A. Gold compounds as therapeutic agents for human diseases. *Metallomics* **2011**, *3*, 863−873.
(10) Gabbiani, C.; Messori, L. Protein targets for anticancer gold compounds: mechanistic inferences. *Anticancer Agents Med. Chem.* **2011**, *11*, 929−939.
(11) Lima, J. C.; Rodriguez, L. Phosphine-gold(I) compounds as anticancer agents: general description and mechanisms of action. *Anticancer Agents Med. Chem.* **2011**, *11*, 921−928.
(12) Rubbiani, R.; Kitanovic, I.; Alborzinia, H.; Can, S.; Kitanovic, A.; Onambele, L. A.; Stefanopoulou, M.; Geldmacher, Y.; Sheldrick, W. S.; Wolber, G.; Prokop, A.; Wolfl, S.; Ott, I. Benzimidazol-2-ylidene gold(I) complexes are thioredoxin reductase inhibitors with multiple antitumor properties. *J. Med. Chem.* **2010**, *53*, 8608−8618.
(13) Rubbiani, R.; Can, S.; Kitanovic, I.; Alborzinia, H.; Stefanopoulou, M.; Kokoschka, M.; Monchgesang, S.; Sheldrick, W. S.; Wolfl, S.; Ott, I. Comparative in vitro evaluation of N-heterocyclic carbene gold(I) complexes of the benzimidazolylidene type. *J. Med. Chem.* **2011**, *54*, 8646−8657.
(14) Schuh, E.; Pfluger, C.; Citta, A.; Folda, A.; Rigobello, M. P.; Bindoli, A.; Casini, A.; Mohr, F. Gold(I) carbene complexes causing thioredoxin 1 and thioredoxin 2 oxidation as potential anticancer agents. *J. Med. Chem.* **2012**, *55*, 5518−5528.
(15) Craig, S.; Gao, L.; Lee, I.; Gray, T.; Berdis, A. J. Gold-containing indoles as anticancer agents that potentiate the cytotoxic effects of ionizing radiation. *J. Med. Chem.* **2012**, *55*, 2437−2451.
(16) Marzano, C.; Gandin, V.; Folda, A.; Scutari, G.; Bindoli, A.; Rigobello, M. P. Inhibition of thioredoxin reductase by auranofin induces apoptosis in cisplatin-resistant human ovarian cancer cells. *Free Radical Biol. Med.* **2007**, *42*, 872−881.
(17) Bhabak, K. P.; Mugesh, G. A synthetic model for the inhibition of glutathione peroxidase by antiarthritic gold compounds. *Inorg. Chem.* **2009**, *48*, 2449−2455.
(18) Chiellini, C.; Casini, A.; Cochet, O.; Gabbiani, C.; Ailhaud, G.; Dani, C.; Messori, L.; Amri, E. Z. The influence of auranofin, a clinically established antiarthritic gold drug, on bone metabolism: analysis of its effects on human multipotent adipose-derived stem cells, taken as a model. *Chem. Biodiversity* **2008**, *5*, 1513−1520.
(19) Gromer, S.; Arscott, L. D.; Williams, C. H., Jr.; Schirmer, R. H.; Becker, K. Human placenta thioredoxin reductase. Isolation of the selenoenzyme, steady state kinetics, and inhibition by therapeutic gold compounds. *J. Biol. Chem.* **1998**, *273*, 20096−20101.
(20) Carlock, M. T.; Shaw, C. F., III; Eidsness, M. K.; Watkins, J. W., II; Elder, R. C. Reactions of auranofin and chloro(triethylphosphine)gold with bovine serum albumin. *Inorg. Chem.* **1986**, *25*, 333−339.
(21) Rackham, O.; Nichols, S. J.; Leedman, P. J.; Berners-Price, S. J.; Filipovska, A. A gold(I) phosphine complex selectively induces apoptosis in breast cancer cells: implications for anticancer therapeutics targeted to mitochondria. *Biochem. Pharmacol.* **2007**, *74*, 992−1002.
(22) Urig, S.; Fritz-Wolf, K.; Reau, R.; Herold-Mende, C.; Toth, K.; Davioud-Charvet, E.; Becker, K. Undressing of phosphine gold(I) complexes as irreversible inhibitors of human disulfide reductases. *Angew. Chem., Int. Ed.* **2006**, *45*, 1881−1886.
(23) Arner, E. S.; Holmgren, A. Physiological functions of thioredoxin and thioredoxin reductase. *Eur. J. Biochem.* **2000**, *267*, 6102−6109.
(24) Lillig, C. H.; Holmgren, A. Thioredoxin and related molecules: from biology to health and disease. *Antioxid. Redox Signaling* **2007**, *9*, 25−47.
(25) Urig, S.; Becker, K. On the potential of thioredoxin reductase inhibitors for cancer therapy. *Semin. Cancer Biol.* **2006**, *16*, 452−465.
(26) Powis, G.; Kirkpatrick, D. L. Thioredoxin signaling as a target for cancer therapy. *Curr. Opin. Pharmacol.* **2007**, *7*, 392−397.
(27) Nguyen, P.; Awwad, R. T.; Smart, D. D.; Spitz, D. R.; Gius, D. Thioredoxin reductase as a novel molecular target for cancer therapy. *Cancer Lett.* **2006**, *236*, 164−174.
(28) Yoo, M. H.; Xu, X. M.; Carlson, B. A.; Gladyshev, V. N.; Hatfield, D. L. Thioredoxin reductase 1 deficiency reverses tumor phenotype and tumorigenicity of lung carcinoma cells. *J. Biol. Chem.* **2006**, *281*, 13005−13008.
(29) Nauser, T.; Steinmann, D.; Koppenol, W. H. Why do proteins use selenocysteine instead of cysteine? *Amino Acids* **2012**, *42*, 39−44.
(30) Ott, I.; Qian, X.; Xu, Y.; Vlecken, D. H.; Marques, I. J.; Kubutat, D.; Will, J.; Sheldrick, W. S.; Jesse, P.; Prokop, A.; Bagowski, C. P. A gold(I) phosphine complex containing a naphthalimide ligand functions as a TrxR inhibiting antiproliferative agent and angiogenesis inhibitor. *J. Med. Chem.* **2009**, *52*, 763−770.
(31) Bindoli, A.; Rigobello, M. P.; Scutari, G.; Gabbiani, C.; Casini, A.; Messori, L. Thioredoxin reductase: A target for gold compounds acting as potential anticancer drugs. *Coord. Chem. Rev.* **2009**, *253*, 1692−1707.
(32) Fritz-Wolf, K.; Urig, S.; Becker, K. The structure of human thioredoxin reductase 1 provides insights into C-terminal rearrangements during catalysis. *J. Mol. Biol.* **2007**, *370*, 116−127.
(33) Viry, E.; Battaglia, E.; Deborde, V.; Muller, T.; Reau, R.; Davioud-Charvet, E.; Bagrel, D. A sugar-modified phosphole gold complex with antiproliferative properties acting as a thioredoxin reductase inhibitor in MCF-7 cells. *ChemMedChem.* **2008**, *3*, 1667−1670.
(34) Ott, I. On the medicinal chemistry of gold complexes as anticancer drugs. *Coord. Chem. Rev.* **2009**, *253*, 1670−1681.

(35) Bhabak, K. P.; Bhuyan, B. J.; Mugesh, G. Bioinorganic and medicinal chemistry: aspects of gold(I)-protein complexes. *Dalton Trans.* **2011**, *40*, 2099−2111.
(36) Fang, J.; Lu, J.; Holmgren, A. Thioredoxin reductase is irreversibly modified by curcumin: a novel molecular mechanism for its anticancer activity. *J. Biol. Chem.* **2005**, *280*, 25284−25290.
(37) Goto, S.; Yoshida, K.; Morikawa, T.; Urata, Y.; Suzuki, K.; Kondo, T. Augmentation of transport for cisplatin-glutathione adduct in cisplatin-resistant cancer cells. *Cancer Res.* **1995**, *55*, 4297−4301.
(38) Seve, P.; Dumontet, C. Chemoresistance in non-small cell lung cancer. *Curr. Med. Chem. Anticancer Agents* **2005**, *5*, 73−88.
(39) Wang, X.; Guo, Z. The role of sulfur in platinum anticancer chemotherapy. *Anticancer Agents Med. Chem.* **2007**, *7*, 19−34.
(40) Ishikawa, T.; Ali-Osman, F. Glutathione-associated cis-diamminedichloroplatinum(II) metabolism and ATP-dependent efflux from leukemia cells. Molecular characterization of glutathione-platinum complex and its biological significance. *J. Biol. Chem.* **1993**, *268*, 20116−20125.
(41) Berners-Price, S. J.; Girard, G. R.; Hill, D. T.; Sutton, B. M.; Jarrett, P. S.; Faucette, L. F.; Johnson, R. K.; Mirabelli, C. K.; Sadler, P. J. Cytotoxicity and antitumor activity of some tetrahedral bis-(diphosphino)gold(I) chelates. *J. Med. Chem.* **1990**, *33*, 1386−1392.
(42) Mirabelli, C. K.; Johnson, R. K.; Sung, C. M.; Faucette, L.; Muirhead, K.; Crooke, S. T. Evaluation of the in vivo antitumor activity and in vitro cytotoxic properties of auranofin, a coordinated gold compound, in murine tumor models. *Cancer Res.* **1985**, *45*, 32−39.
(43) Massague, J. G1 cell-cycle control and cancer. *Nature* **2004**, *432*, 298−306.
(44) Yoo, M. H.; Xu, X. M.; Carlson, B. A.; Patterson, A. D.; Gladyshev, V. N.; Hatfield, D. L. Targeting thioredoxin reductase 1 reduction in cancer cells inhibits self-sufficient growth and DNA replication. *PLoS One* **2007**, *2*, e1112.
(45) Mochizuki, M.; Kwon, Y. W.; Yodoi, J.; Masutani, H. Thioredoxin regulates cell cycle via the ERK1/2-cyclin D1 pathway. *Antioxid. Redox Signaling* **2009**, *11*, 2957−2971.
(46) Cox, A. G.; Brown, K. K.; Arner, E. S. J.; Hampton, M. B. The thioredoxin reductase inhibitor auranofin triggers apoptosis through a Bax/Bak-dependent process that involves peroxiredoxin 3 oxidation. *Biochem. Pharmacol.* **2008**, *76*, 1097−1109.
(47) Rigobello, M. P.; Scutari, G.; Boscolo, R.; Bindoli, A. Induction of mitochondrial permeability transition by auranofin, a gold(I)-phosphine derivative. *Br. J. Pharmacol.* **2002**, *136*, 1162−1168.
(48) Rigobello, M. P.; Scutari, G.; Folda, A.; Bindoli, A. Mitochondrial thioredoxin reductase inhibition by gold(I) compounds and concurrent stimulation of permeability transition and release of cytochrome c. *Biochem. Pharmacol.* **2004**, *67*, 689−696.
(49) Park, S. J.; Kim, I. S. The role of p38 MAPK activation in auranofin-induced apoptosis of human promyelocytic leukaemia HL-60 cells. *Br. J. Pharmacol.* **2005**, *146*, 506−513.
(50) Saitoh, M.; Nishitoh, H.; Fujii, M.; Takeda, K.; Tobiume, K.; Sawada, Y.; Kawabata, M.; Miyazono, K.; Ichijo, H. Mammalian thioredoxin is a direct inhibitor of apoptosis signal-regulating kinase (ASK) 1. *EMBO J.* **1998**, *17*, 2596−2606.
(51) Berggren, M.; Gallegos, A.; Gasdaska, J. R.; Gasdaska, P. Y.; Warneke, J.; Powis, G. Thioredoxin and thioredoxin reductase gene expression in human tumors and cell lines, and the effects of serum stimulation and hypoxia. *Anticancer Res.* **1996**, *16*, 3459−3466.
(52) Urig, S.; Lieske, J.; Fritz-Wolf, K.; Irmler, A.; Becker, K. Truncated mutants of human thioredoxin reductase 1 do not exhibit glutathione reductase activity. *FEBS Lett.* **2006**, *580*, 3595−3600.
(53) Hosoya-Matsuda, N.; Inoue, K.; Hisabori, T. Roles of thioredoxins in the obligate anaerobic green sulfur photosynthetic bacterium *Chlorobaculum tepidum*. *Mol. Plant.* **2009**, *2*, 336−343.
(54) King, A. R.; Dotsey, E. Y.; Lodola, A.; Jung, K. M.; Ghomian, A.; Qiu, Y.; Fu, J.; Mor, M.; Piomelli, D. Discovery of potent and reversible monoacylglycerol lipase inhibitors. *Chem. Biol.* **2009**, *16*, 1045−1052.
(55) Liu, T.; Toriyabe, Y.; Kazak, M.; Berkman, C. E. Pseudoirreversible inhibition of prostate-specific membrane antigen by phosphoramidate peptidomimetics. *Biochemistry* **2008**, *47*, 12658−12660.
(56) Kikuchi, Y.; Kizawa, I.; Oomori, K.; Miyauchi, M.; Kita, T.; Sugita, M.; Tenjin, Y.; Kato, K. Establishment of a human ovarian cancer cell line capable of forming ascites in nude mice and effects of tranexamic acid on cell proliferation and ascites formation. *Cancer Res.* **1987**, *47*, 592−596.
(57) Zhang, Y. F., J.; Jia, Y.; Wang, X.; Zhang, L.; Liu, C.; Fang, H.; Xu, W. Development of tetrahydroisoquinoline-based hydroxamic acid derivatives: potent histone deacetylase inhibitors with marked in vitro and in vivo antitumor activitie. *J. Med. Chem.* **2011**, *54*, 2823−2838.